

A Journal of the Gesellschaft Deutscher Chemiker

Angewandte Chemie

GDCh

International Edition

www.angewandte.org

Accepted Article

Title: Photoinduced Trifluoromethylation of Arenes and Heteroarenes Catalyzed by High-Valent Nickel Complexes

Authors: Shubham Deolka, Ramadoss Govindarajan, Eugene Khaskin, Robert R. Fayzullin, Michael C. Roy, and Julia Khusnutdinova

This manuscript has been accepted after peer review and appears as an Accepted Article online prior to editing, proofing, and formal publication of the final Version of Record (VoR). This work is currently citable by using the Digital Object Identifier (DOI) given below. The VoR will be published online in Early View as soon as possible and may be different to this Accepted Article as a result of editing. Readers should obtain the VoR from the journal website shown below when it is published to ensure accuracy of information. The authors are responsible for the content of this Accepted Article.

To be cited as: *Angew. Chem. Int. Ed.* 10.1002/anie.202109953

Link to VoR: <https://doi.org/10.1002/anie.202109953>

RESEARCH ARTICLE

Photoinduced Trifluoromethylation of Arenes and Heteroarenes Catalyzed by High-Valent Nickel Complexes

Shubham Deolka,^[a] Ramadoss Govindarajan,^[a] Eugene Khaskin,^[a] Robert R. Fayzullin,^[b] Michael C. Roy,^[a] and Julia R. Khusnutdinova*^[a]

[a] S. Deolka, R. Govindarajan, E. Khaskin, M. C. Roy, J. R. Khusnutdinova
Okinawa Institute of Science and Technology Graduate University
Onna-son, Kunigami-gun, Okinawa, Japan, 904-0495
E-mail: juliak@oist.jp

[b] R. R. Fayzullin
Abuzov Institute of Organic and Physical Chemistry, FRC Kazan Scientific Center of RAS
8 Arbuzov Street, Kazan 420088, Russian Federation

Supporting information for this article is given via a link at the end of the document.

Abstract: We describe a series of air-stable Ni^{III} complexes supported by a simple, robust naphthyridine-based ligand. Access to the high valent oxidation state is enabled by the CF₃ ligands on the nickel, while the naphthyridine exhibits either a monodentate or bidentate coordination mode that depends on the oxidation state and sterics, and enables facile aerobic oxidation of Ni^{II} to Ni^{III}. These Ni^{III} complexes act as efficient photoredox catalysts for C(sp²)-H bond trifluoromethylation reactions of (hetero)arenes using versatile synthetic protocols. This blue LED light-mediated catalytic protocol proceeds via a radical pathway and demonstrates potential in the late-stage functionalization of drug analogs.

Introduction

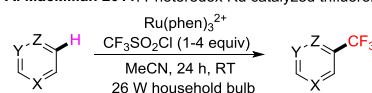
Recently, nickel has emerged as a significantly cheaper alternative to palladium in a wide array of catalytic reactions.^[1] Many reactions that were first catalyzed by expensive noble metals catalysts, such as cross-coupling,^[2] nucleophilic allylation,^[3] and fluorination/trifluoromethylation reactions among others,^[4] can now all be done via nickel, albeit normally at greater catalyst loading.^[5] These catalytic reactions are often proposed to proceed via high valent Ni^{III}/Ni^{IV} intermediates.^[6] In the last few years, several reports have suggested that complexes that have access to high valent oxidation states of nickel, can end up being competent catalysts in C-O,^[7] C-C^[8] bond formation and C-H bond functionalization.^[9] However, a general approach for the accessibility/formation of high valent nickel complexes is still lacking due to their low stability.^[10]

Arene trifluoromethylation has recently emerged as a powerful strategy for modifying advanced intermediates,^[11] and even active pharmaceuticals,^[12] with a functional group that can significantly change the pharmacokinetics of a known drug^[13] and assists in its passage through the blood/brain barrier.^[14] A seminal report by MacMillan showed that a second-row metal Ru photosensitizer was able to catalytically install the CF₃ group at good efficiency using a cheap CF₃ source (Figure 1).^[15] However, there are only a few examples of inexpensive first-row transition metals being used as catalysts for arene trifluoromethylation.^[10c, 16] An important consideration for developing a practically applicable catalyst is the use of a simple and inexpensive ligand and trifluoromethyl group source.

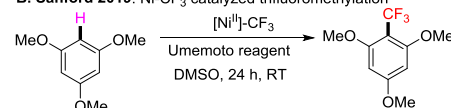
There are several recent reports where Ni complexes were utilized for trifluoromethylation, all suggesting that a higher Ni oxidation state is required for CF₃ modification. Vicić and coworkers showed that ArNi^{II}CF₃ was unfeasible for reductive elimination (RE)^[17]. Later, Nebra and coworkers designed a high valent Ni^{IV} complex where stoichiometric trifluoromethylation was shown to occur via reductive elimination.^[18] There, the Ni complex was used as a stoichiometric reagent and a CF₃ source in the presence of excess substrate. Finally, the Sanford group has recently reported that a pyrazolyl borate supported complex catalyzed trifluoromethylation of arenes via a Ni^{IV} intermediate and a fluoro-modified Umemoto reagent.^[16a] Similar catalytic activity was reported recently by the Vicić group using solvated Ni complexes.^[19] In the Sanford and Vicić protocols, the Umemoto reagent was used as the limiting reagent in the presence of the excess substrate. This is not ideal in the case of an expensive heterocycle substrate as it results in low conversion.

Although feasibility in catalysis was demonstrated, Ni-catalyzed trifluoromethylation examples currently lack the versatility of precious metal protocols and do not attempt to utilize a photochemical approach such as that demonstrated by MacMillan. In particular, despite the recent surge of interest in the photochemistry of organometallic nickel complexes, examples of Ni-catalyzed, photoinduced C-H bond functionalization reactions remain scarce,^[20] and no examples of photo-induced, base-metal, trifluoromethylation catalysts are currently known.

A. MacMillan 2011: Photoredox Ru catalyzed trifluoromethylation



B. Sanford 2019: Ni-CF₃ catalyzed trifluoromethylation



C. This work: Photoinduced trifluoromethylation catalyzed by high-valent Ni

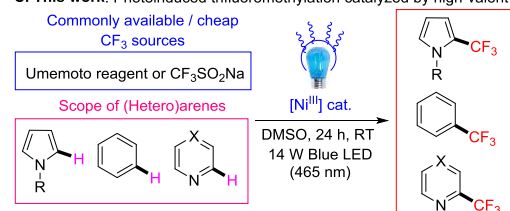


Figure 1. Catalytic trifluoromethylation of (hetero)arenes.

RESEARCH ARTICLE

A major theme of our group's research consists of designing bimetallic systems with a naphthyridine ligand core, resulting in complexes that often reveal mechanistic insights into catalytic processes.^[21] We recently began to examine nickel as it is active in a number of coupling reactions, including trifluoromethylation. During an evaluation of a series of alkyl-substituted naphthyridine ligands, we found that bis-trifluoromethyl nickel(II) complexes chelated by simple naphthyridines are easily oxidized by air as the sole oxidant to produce air-stable and isolable Ni^{III} bis-trifluoromethyl complexes. This is the first example of facile aerobic oxidation of an organometallic Ni complex to give well-defined, isolated Ni^{III} species.

Further exploring the chemistry of these unusual, bidentate-mode coordinated naphthyridine complexes, we found that they were capable of trifluoromethylating arenes even under air when irradiated with blue LED light. Inspired by the above reports on high-valent nickel catalysis and photoredox mediated Ru trifluoromethylation, we were able to extend their chemistry to achieve efficient photocatalytic trifluoromethylation via two alternative protocols, using either a cheap CF₃SO₂Na, or the more expensive but also commercially available Umemoto (non-modified) reagent as a CF₃ source (Figure 1).

This result is to the best of our knowledge, the first report of a Ni-catalyzed photoinduced trifluoromethylation. Under the optimized procedure, our TONs are also an order of magnitude higher than those achieved in the earlier Ni protocol.

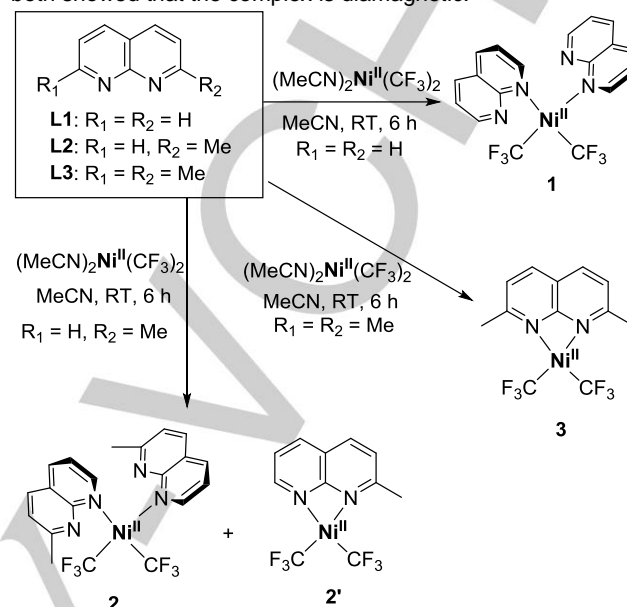
Thus, we developed a system with a cheap and readily available ligand and CF₃ reagent set, shows photoinduced reactivity, and does not require a 2nd/3rd-row transition metal. Our preliminary mechanistic studies show that CF₃ radical formation occurs during catalysis, and that it is promoted by blue LED light irradiation (465 nm) under mild conditions.

Results and Discussion

Ligand design and synthesis of Ni^{II}/Ni^{III} bis-trifluoromethyl complexes. We focused our attention on Ni(MeCN)₂(CF₃)₂ as a stable and easily accessible precursor that could potentially stabilize higher oxidation states of Ni when combined with N-donor ligands. Treating Ni(MeCN)₂(CF₃)₂ with 2 equiv. of 1,8-naphthyridine ligand (**L1**) (Scheme 1) formed the yellow color complex **1**, which was isolated in 71% yield and characterized by ¹H NMR, UV-vis, FT-IR, high-resolution mass spectrometry (HRMS), and single-crystal X-ray diffraction (SC-XRD). The ¹H NMR spectrum of **1** displayed broadened resonances in the aromatic region that could not be fully resolved even at –80 °C, suggesting fluxional behavior (see below).

The X-ray structure of **1** revealed that there are two independent halves of two molecules in the asymmetric cell (*Z'* = ½ + ½), where each Ni atom is situated on the second-order rotational axis and supported by two monodentate **L1** ligands, with one Ni center featuring almost ideal square planar geometry with $\tau_4 = \tau_4' = 0.03$ (Figure 2a) and another Ni center exhibiting slight distortion from square planar geometry with $\tau_4 = \tau_4' = 0.16$.^[22] This is also manifested in the different *trans*-C–Ni–N angles in both structures: while the square planar geometry is characterized by an almost ideal C1–Ni1–N11ⁱ angle of 178.13(6)°, the analogous angle in the distorted square planar complex is 168.77(6)°, showing significant deviation from planarity. Interestingly, deviation from planarity was also reported by Vicić and co-

workers for their bipyridine-supported Ni^{II}(CF₃)₂ complex and was attributed to sterics.^[23] We hypothesized that the NMR broadening of **1** likely arises due to the low interconversion barrier between the square planar and distorted geometries, although other types of ligand exchange cannot be excluded (*vide infra*). A solid state and a solution (Evans method) magnetic moment measurement both showed that the complex is diamagnetic.



Scheme 1. Synthesis of Ni^{II}(CF₃)₂ complexes **1-3** supported by naphthyridine ligands.

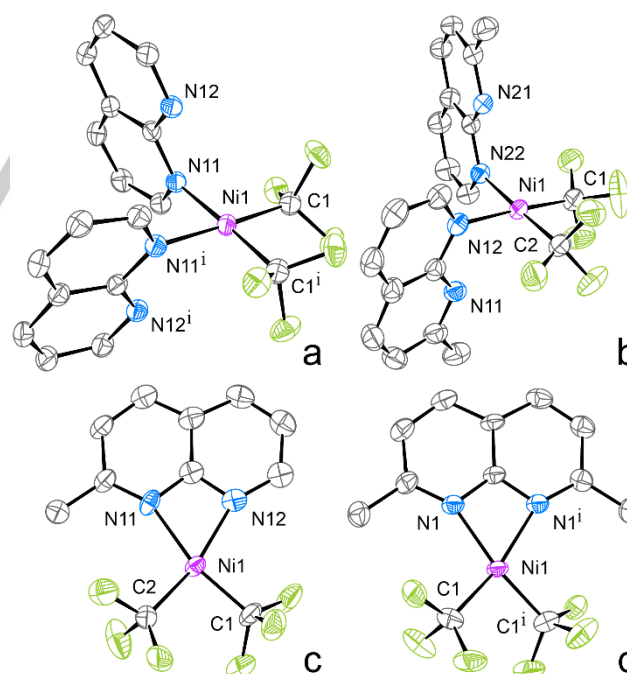


Figure 2. ORTEP of **1** (a), **2** (b), **2'** (c), and **3** (d) at the 60% (a, b, and d) or 30% (c) probability level. The second independent molecule for **1** and **2'**, solvent molecule for **2**, and hydrogen atoms are omitted for clarity.^[24]

RESEARCH ARTICLE

To induce bidentate ligand coordination to the Ni^{II} metal center, we then utilized monomethyl and dimethyl-substituted naphthyridine ligands, **L2** and **L3**. Reacting **L2** with Ni(MeCN)₂(CF₃)₂ at room temperature (RT) gave yellow color complex **2**. Two types of crystals were obtained, **2** and **2'**, by crystallization from an acetone/pentane solvent mixture and *m*-xylene, respectively (Figure 2b, c). Complex **2**, crystallized from acetone/pentane as a 1:1 acetone solvate, showed an almost ideal square planar Ni^{II} atom bound to two monodentate **L2** ligands ($\tau_4 = 0.04$, $\tau_4' = 0.03$), while N-atoms next to the two ortho-Me groups in **L2** remained non-coordinated. The XRD analysis for crystals of **2'** obtained from a non-polar *m*-xylene allowed to establish atom connectivity and confirmed a bidentate coordination mode of only one **L2** ligand per Ni center, showing a distorted square planar geometry ($\tau_4 = \tau_4' = 0.21$ -0.22). The ¹H and ¹⁹F NMR spectra in CD₂Cl₂ solution showed broadened signals at RT, suggesting that chemical exchange likely occurs in solution. At -80 °C, signals of CF₃ in the ¹⁹F NMR spectrum and singlets of Me groups of **L2** in the ¹H NMR spectrum partially resolved, confirming that the complex was present as a mixture of two main components, presumably the 2:1 and 1:1 complexes **2** and **2'**.

By contrast, the even more sterically hindered bis-Me **L3** was able to react in a clean 1:1 ratio with the precursor to provide facile access to the bidentate yellow complex **3**, which displayed a well-resolved NMR spectrum featuring sharp peaks even at room temperature. Isolated complex **3** was characterized by NMR, FT-IR, UV-vis, ESI-HRMS, and elemental analysis. The strained bidentate coordination of **L3** forming a four-membered chelate cycle is manifested in the small N1–Ni1–N1ⁱ angle of 67.09(13)° (Figure 2d). The geometry around the Ni atom is distorted square planar ($\tau_4 = \tau_4' = 0.23$) with a C1–Ni1–N1ⁱ angle of 163.59(12)°.

Next, we examined whether **1-3** can react with 1e⁻/2e⁻ oxidants to yield Ni^{III}/Ni^{IV} products. Recent studies by Mirica, Vicić, and Sanford have shown that Ni^{II} organometallic complexes can react with outer-sphere 1e⁻/2e⁻ oxidants to form high-valent Ni^{III} or Ni^{IV} complexes. The cyclic voltammograms (CV) for complexes **1**, **2**, and **3** showed chemically reversible oxidation waves at the anodic peak potentials E_{pa} 0.492, 0.468, and 0.448 V vs. Fc/Fc⁺, respectively, with a large peak-to-peak separation between forward and reverse waves (ΔE_p in a range of 0.612-0.695 V) indicative of significant structural reorganization during oxidation (Table S1, Figure 3). Surprisingly, we found that solution of complex **3** was air-sensitive even in the absence of added oxidants leading to the formation of a purple solution containing paramagnetic oxidation product as confirmed by NMR and EPR spectroscopy. Upon further optimization, we found that simply stirring complex **3** under air with a NaBF₄ salt additive in MeOH solution gave the deep-purple complex **3a**, which was isolated in 42% yield and characterized by XRD (Figure 4b). According to XRD, **3a** is a monocationic complex showing a tetragonally distorted octahedral geometry around the Ni atom, with two **L3** ligands bound in a bidentate fashion and the two CF₃ groups *cis* to each other. The axial Ni–N distances (2.1665(12)-2.1937(12) Å) are significantly elongated compared to the equatorial Ni–N distances (2.0340(12)-2.0343(13) Å), consistent with a Jahn–Teller distorted Ni^{III} center. The Ni–C bond distances in **3a** (1.9306(16)-1.9364(15) Å) are slightly longer compared to the corresponding Ni^{II} complex **3** (1.879(3) Å).

The low yield is a direct result of requiring a sacrificial **L3** ligand from another complex of **3**. When the reaction was

performed in presence of 1 equiv of **L3**, the isolated yield increased to 75%. Complex **3a** was characterized by electrospray ionization high-resolution mass spectrometry (ESI-HRMS), UV-vis, FT-IR, and EPR spectroscopy, and elemental analysis. We found that **3a** is stable under air for months without apparent decomposition.

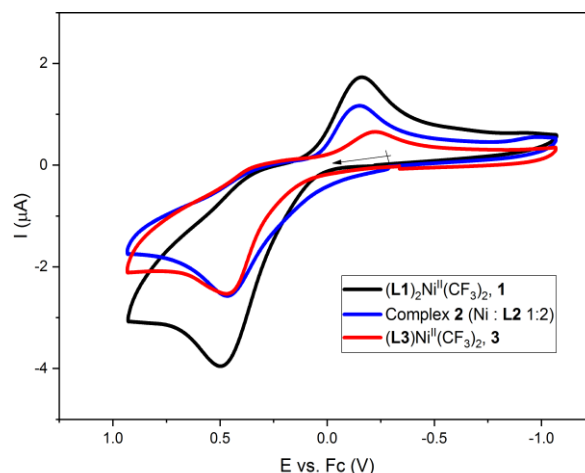
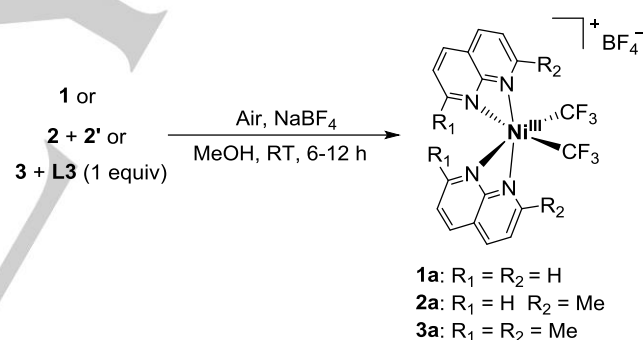


Figure 3. Cyclic voltammograms of complexes **1** (black), **2** (blue), and **3** (red). Conditions: 0.1M ⁿBu₄NBF₄/MeCN solutions at RT, scan rate 0.1 V s⁻¹, 1.6 mm Pt disk electrode, the arrow indicates the initial scan direction. Complex **2** is obtained by reacting 2 equiv of **L2** with Ni precursor.



Scheme 2. Synthesis of Ni^{III}-CF₃ complexes **1a-3a**.

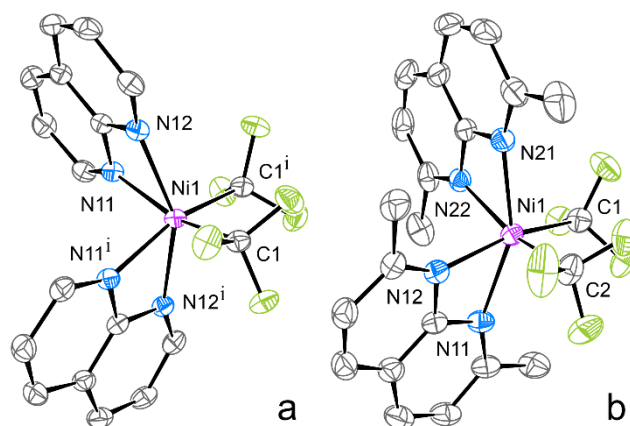


Figure 4. ORTEP of **1a** (a) and **3a** (b) at 60% probability level. Counterion BF₄⁻ and hydrogen atoms are omitted for clarity.^[24]

RESEARCH ARTICLE

The X-band EPR spectrum of **3a** ("PrCN/EtCN glass, 94 K) exhibits an axial signal with $g_{\perp} = 2.203$ and $g_{\parallel} = 2.020$ featuring superhyperfine splitting from two N-atoms along g_z ($A_N = 17.8$ G) (Figure 5). Significant g anisotropy ($\Delta g = g_{\perp} - g_{\parallel} = 0.183$) and relatively high average g value ($g_{\text{ave}} = 2.142$) suggest significant localization of the spin density at the Ni center consistent with DFT-calculated spin density distribution (Figure 6).^[8, 25]

We next investigated aerobic oxidation of the two other $\text{Ni}^{\text{II}}(\text{CF}_3)_2$ complexes **1** and **2** in the presence of NaBF_4 (Scheme 2). As these complexes were obtained by reacting Ni precursor with 2 equiv of ligand **L1** or **L2**, no additional ligand was added (in the case of complex **2**, an undetermined amount of free ligand **L2** was present in the reaction mixture before oxidation). We found that these complexes also reacted with air to form Ni^{III} complexes, and reddish-purple complex **1a** and purple complex **2a** were isolated from MeOH solutions in 74% and 57% yields respectively, and characterized by EPR, FT-IR, UV-vis, ESI-HRMS, and elemental analysis. Complex **1a** was also characterized by SC-XRD (Figure 4a), showing a similar distorted octahedral geometry with an elongated axial Ni–N distances (2.1826(11) Å) as compared to equatorial Ni–N distances (2.0248(12) Å). The Ni–C distances in **1a** (1.9373(14) Å) are also elongated as compared to **1** (Ni–C 1.9023(16) and 1.8977(16) Å for the first and second molecules), reflecting a similar trend as in complexes **3a** and **3**. The rest of the spectroscopic features were consistent with the structure of **1a** and **3a**. The magnetic moments in CD_3CN solution measured by the Evans method for complexes **1a**, **2a**, and **3a** were determined to be 2.04, 1.87, and 1.95 μ_B , respectively, corresponding to one unpaired electron. The EPR spectrum of complex **1a** revealed a nearly axial signal similar to **3a** with g_{ave} of 2.141 ($g_x = 2.200$, $g_y = 2.183$, $g_z = 2.0202$) and showing superhyperfine splitting from two N-atoms in the g_z component ($A_N = 16.8$ G) (Figure S34), while the signal for **2a** was broadened and poorly resolved probably due to low symmetry and possible isomer formation (Figure S35).

Considering that aerobic oxidation is often proposed to involve superoxide intermediates, we attempted to detect possible metal-superoxide species using DMPO as a spin trap (Figure 7). Indeed, exposure of **3** to air in MeOH solution in the presence of DMPO gave rise to a new signal whose superhyperfine splitting constants ($A_N = 13.57$ G, $A_H = 8.21$ G, $g = 2.008$) resemble those reported for detected or proposed metal-superoxide species in aerobic oxidation of first-row transition metals such as Co,^[26] Cu,^[27] or Ni.^[28]

Overall, these results show that simple naphthyridine-based ligands induce facile aerobic oxidation and stabilization of Ni^{III} complexes. Complex multi-chelating tri- and tetradentate ligands were not necessary for the formation of stable Ni^{III} complexes, contrary to the commonly used strategy reported in the literature for stabilization of high valent Ni species, and even with a simple naphthyridine ligand, selective aerobic oxidation was achieved. We believe that the highly strained coordination and small bite angle of the naphthyridine-based ligands, resulting in unsymmetrical coordination with notably different Ni–N distances, make them suitable for stabilization of Jahn–Teller distorted Ni^{III} centers leading to such unexpected oxidation behavior and the trifluoromethylation reactivity presented below.

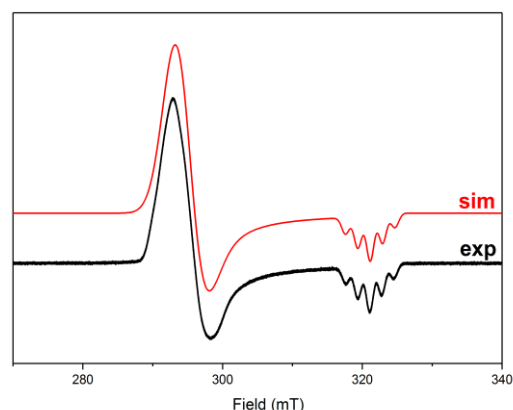


Figure 5. Experimental (black line) and simulated (red line) EPR spectra of **3a** in "PrCN–EtCN glass (1:1) at 94 K. Simulation parameters: $g_{\perp} = 2.203$, $g_{\parallel} = 2.020$, $A_{N,zz} = 17.86$ G.

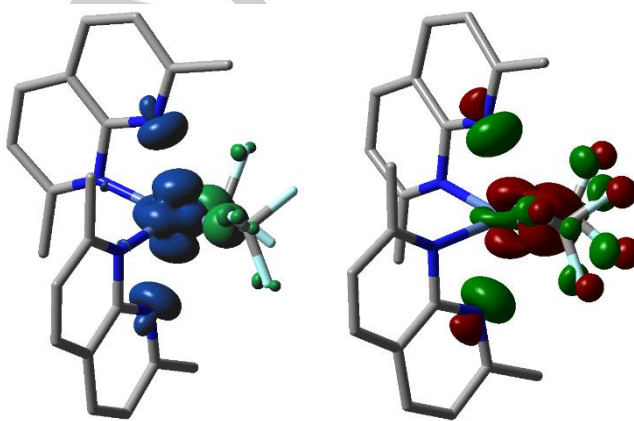


Figure 6. Calculated spin density (left; isovalue 0.004) and singly occupied molecular orbital (right; isovalue 0.06) for **3a** cation $[(\text{L}3)_2\text{Ni}(\text{CF}_3)_2]^+$ in the gas phase. The geometry was optimized using ωB97XD functional^[29] and def2tzvp basis set^[30] for all elements.

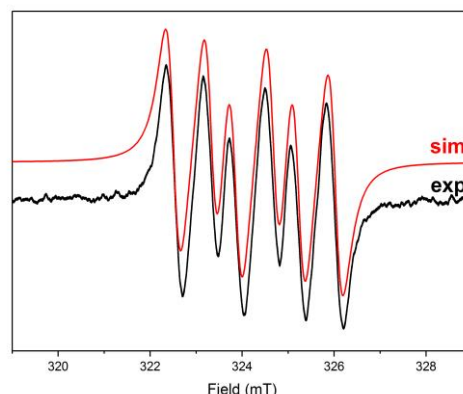
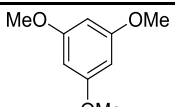
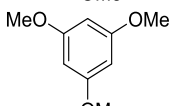
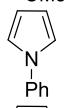
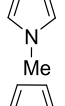
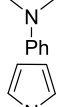
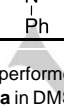


Figure 7. Experimental (black line) and simulated (red line) EPR spectra of the solution of **3** exposed to air for 4 min at RT in MeOH in the presence of NaBF_4 and DMPO spin trap. Simulation parameters: $A_N = 13.57$ G; $A_H = 8.21$ G, $g = 2.008$.

RESEARCH ARTICLE

Stoichiometric trifluoromethylation. The above results meant that we now had access to three air-stable $\text{Ni}^{\text{III}}\text{-CF}_3$ complexes. Based on literature analogs, we anticipated that these complexes might show propensity to undergo homolysis of the $\text{Ni}^{\text{III}}\text{-CF}_3$ bond, leading to CF_3 radical formation, which could ultimately be applied for $\text{C}(\text{sp}^2)\text{-H}$ bond trifluoromethylation. For example, transient formation of unstable $\text{Ni}^{\text{III}}(\text{CF}_3)_2$ complexes with terpyridine ligand has been reported by Vicic upon oxidation of the corresponding $\text{Ni}^{\text{II}}(\text{CF}_3)_2$ precursor with ferrocenium.^[25] This complex was shown to be unstable and highly reactive, leading to immediate $\text{Ni}\text{-CF}_3$ bond homolysis, and was not used in stoichiometric or catalytic trifluoromethylation reactions. Transient Ni^{III} species were proposed in other trifluoromethylation protocols using the Togni reagent or Langlois reagent, however, they were not detected experimentally.^[10c, 16b] Soper and co-workers reported light-induced $\text{Co}^{\text{III}}\text{-CF}_3$ bond homolysis, however, only stoichiometric trifluoromethylation of arene was observed and no catalytic transformation was reported.^[31] Having isolated $\text{Ni}^{\text{III}}(\text{CF}_3)_2$ complexes **1a-3a**, we aimed to induce CF_3 radical formation in a controlled way, in particular, using light to trigger bond homolysis, and utilize it for stoichiometric or catalytic C-H bond trifluoromethylation.

Table 1. Stoichiometric C-H bond trifluoromethylation by **3a**.^[a]

Entry	Substrate	Conditions	Yield [%]
1		Ambient light	< 5
2		Blue LED (465 nm)	16
3		Blue LED	40
4		Blue LED	58
5		Blue LED $\text{K}_2\text{S}_2\text{O}_8$ (1 equiv)	71
6		Blue LED $t\text{BuOOH}$ (1 equiv)	80

[a] The reactions were performed under air for 24 hours using 1 equiv of substrate and 1 equiv of **3a** in DMSO at RT under blue LED light (465 nm) unless indicated otherwise. The yields were determined by ^{19}F NMR based on integration against α,α,α -trifluorotoluene as a standard.

Our first attempt, the reaction of 1,3,5-trimethoxybenzene under ambient light, afforded only a trace amount of mono-trifluoromethylated product. Inspired by previous reports of light-induced metal-carbon bond homolysis in Pd^{III} complexes^[32] and the synthetic utility of photochemical trifluoromethylation reported by the MacMillan group,^[15] we then attempted this transformation under blue LED light (465 nm). Exposing **3a** and 1,3,5-trimethoxybenzene to blue LED light afforded the monotrifluoromethylated product in 16% yield, showing that

photoirradiation improved the reaction outcome (Table 1, entry 2). Ultimately, we found that the transformation was more effective in the case of pyrroles, giving moderate yields of 40-58% in the stoichiometric reaction for N-substituted pyrroles (Table 1, entries 3-4). Interestingly, adding an oxidant^[33] to the typical pyrrole C-H trifluoromethylation reaction (entries 5-6) gave much larger yields and suggested that the reaction may not have been strictly stoichiometric, which ultimately led us to develop a catalytic version of this transformation (*vide infra*).

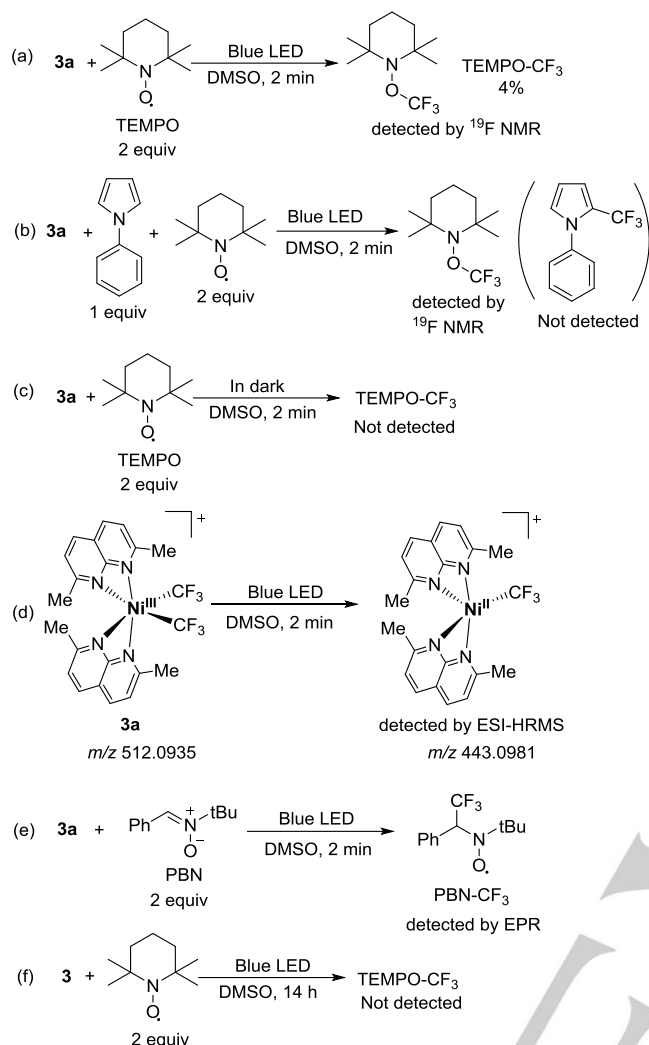
To confirm that light-induced CF_3 radical formation is involved in the stoichiometric reactivity, we exposed a DMSO solution of complex **3a** and the TEMPO radical trap to blue LED irradiation at RT. NMR analysis showed the formation of the TEMPO- CF_3 adduct after just several minutes of irradiation (Scheme 3, a). Similarly, the TEMPO- CF_3 adduct was also observed when a solution of **3a** and TEMPO was irradiated in the presence of a substrate, N-phenylpyrrole, where at the same time, formation of the trifluoromethylation product was suppressed (Scheme 3, b). No TEMPO- CF_3 radical was observed when **3a** was reacted with TEMPO in the absence of light showing that the bond homolysis at RT is induced by irradiation (Scheme 3, c). The ESI-HRMS analysis of complex **3a** solution after irradiation with blue LED in the absence of TEMPO showed the presence of a signal corresponding to a $[(\text{L}3)_2\text{Ni}^{\text{II}}\text{CF}_3]^+$ species (m/z 443.0981), which is likely to result from a $\text{Ni}^{\text{III}}\text{-CF}_3$ bond homolyses (Scheme 3, d).

In addition, we performed spin trapping experiments using a solution of **3a** in the presence of PBN as a radical trap. The EPR analysis of the reaction mixture confirmed the formation of a CF_3 -PBN adduct, which was detected by EPR spectroscopy ($A_N = 14.28$ G, $A_H = 2.11$ G, $A_F = 1.54$ G (CF_3), $g = 2.007$) after several minutes of irradiation with blue LED light (Figure 8 and Scheme 3, e). The simulated spectrum and superhyperfine splitting constants are in good agreement with literature data for the PBN- CF_3 radical adduct.^{[34],[25]}

Finally, we checked the reactivity of a parent $\text{Ni}^{\text{II}}(\text{CF}_3)_2$ complex in the absence of oxidant/air. However, exposure of Ni^{II} complex **3** to blue LED light in the presence of TEMPO did not lead to TEMPO- CF_3 formation, suggesting that a higher oxidation state is necessary for CF_3 radical formation (Scheme 3, f).

Overall, these results show that light-induced homolysis of the $\text{Ni}^{\text{III}}\text{-CF}_3$ bond in complex **3a** results in the formation of a CF_3 radical, which then participates in $\text{C}(\text{sp}^2)\text{-H}$ bond trifluoromethylation. This reaction is enhanced by the addition of oxidants.

RESEARCH ARTICLE



Scheme 3. Ni–CF₃ bond homolysis in **3a**. For experiments under light irradiation, 14 W blue LED lamp (465 nm) was used.

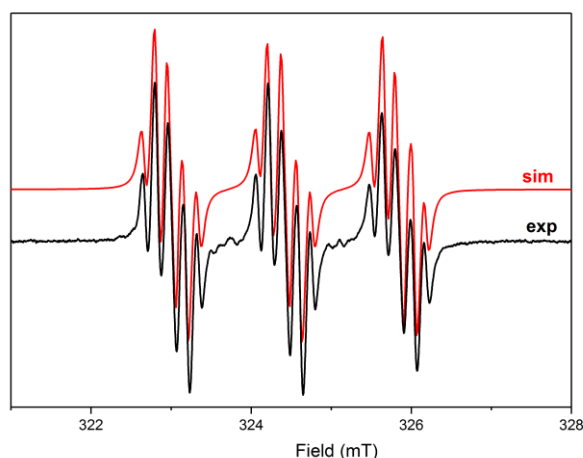
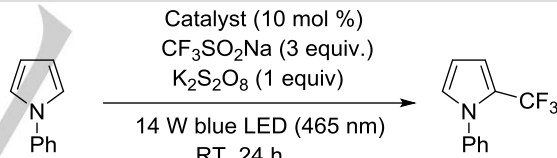


Figure 8. Experimental (black line) and simulated (red line) EPR spectra of the solution of **3a** exposed blue LED irradiation for 2 min in the presence of PBN spin trap in DMSO solution. Simulation parameters: $A_N = 14.28$ G; $A_H = 2.11$ G, $A_F = 1.54$, $g = 2.0075$.

Catalytic trifluoromethylation. After the observation that added oxidants improved the reaction outcome, we believed that we could develop a workable catalytic protocol for selective C–H trifluoromethylation of heteroarenes with a cheap oxidant and a readily available CF₃-source. Considering the stability of our Ni^{III} complexes under air, we were also looking to possibly develop a robust system for photoinduced trifluoromethylation that could work under ambient atmosphere.

Using 10 mol% of **3a** and N-phenylpyrrole as a substrate in the presence of 3 equiv of sodium triflinite, CF₃SO₂Na, as a CF₃ source, and 1 equiv of K₂S₂O₈ as an oxidant under blue LED irradiation, afforded the mono-trifluoromethylated pyrrole product in 85% yield after 24 h at RT (Table 2, entry 1), by contrast to the 16% yield obtained in the presence of ambient light under otherwise identical conditions. The yield did not change dramatically in the presence of K₂HPO₄ base (87% yield) (entry 3). Catalyst **3a** was the most efficient compared to **1a** (40%) and **2a** (67%) (entries 1, 4, and 5). As expected, under these conditions the background, non-photoinduced radical trifluoromethylation also occurred;^[33] however, the reaction in the absence of Ni complexes afforded only 30% of trifluoromethylation product, indicating that the presence of **3a** leads to significantly higher yields and more efficient trifluoromethylation (entry 6). Interestingly, when the reaction was performed under an N₂ atmosphere, the yield decreased to 62% (entry 7). Considering that complex **3a** was formed from **3** under aerobic conditions, we hypothesize that air could play a role in recycling the catalytically relevant Ni^{III} species. Other solvents, MeOH and MeCN, led to lower yields (entries 8 and 9).

Table 2. Optimization of reaction conditions for C–H trifluoromethylation using CF₃SO₂Na/oxidant as a CF₃-source.^[a]

<div style="text-align: center;">  </div>			
Entry	Catalyst	Solvent, conditions	Yield [%] ^[b]
1	3a	DMSO	85
2	3a	Ambient light, DMSO	16
3	3a	K ₂ HPO ₄ (1 equiv), DMSO	87
4	1a	DMSO	40
5	2a	DMSO	67
6	none	DMSO	30
7	3a	DMSO, under N ₂	62
8	3a	MeOH	15
9	3a	MeCN	6

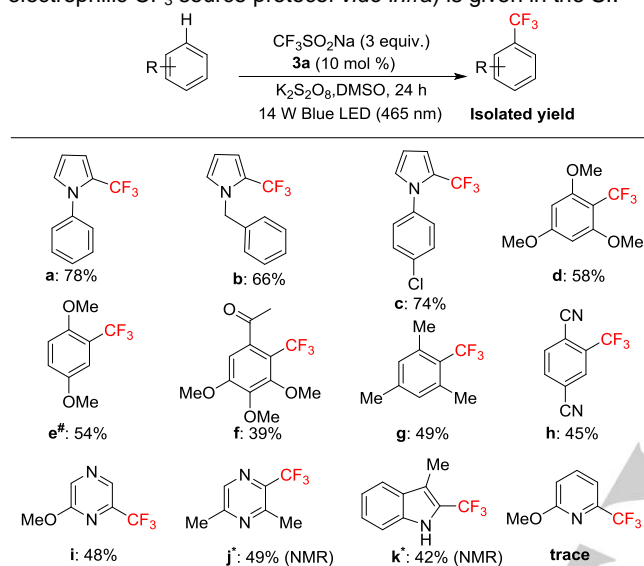
[a] The reaction was performed under air unless indicated otherwise. [a] NMR yield was based on integration against α,α,α-trifluorotoluene as an internal standard.

Other oxidants were also tested in this reaction, however, using KHSO₅–K₂SO₄ led to a notably lower yield (32%), while ^tBuOOH resulted in an exothermic reaction. Another

RESEARCH ARTICLE

trifluoromethyl group source, $\text{CF}_3\text{SO}_2\text{Cl}$ in the presence of $\text{K}_2\text{S}_2\text{O}_8$, was also less efficient, giving a 40% NMR yield of the trifluoromethylation product (see SI).

The optimized protocol with **3a** was used for a number of pyrroles (Scheme 4, entries a-c), pyrimidines (entries i-j), and some electron-rich simple arenes (entries d-h) successfully to give C-H trifluoromethylation products in ca. 40–78% isolated yields. However, the protocol was not successful in the case of relatively more electron-poor pyridines and other electron-deficient arenes, and non-substituted indole gave a mixture of 2- and 3-trifluoromethylated isomers (see SI, Scheme S7). A further list of substrates that we found worked poorly under this (and the electrophilic CF_3 source protocol *vide infra*) is given in the SI.



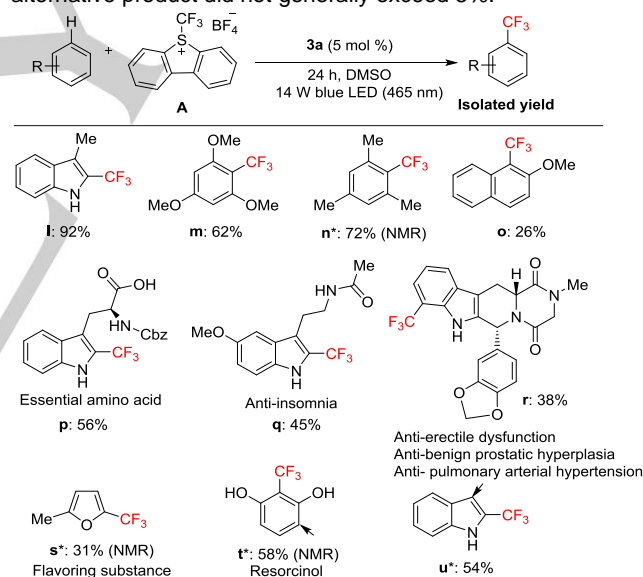
Scheme 4. Scope of radical trifluoromethylation catalyzed by **3a** in the presence of $\text{CF}_3\text{SO}_2\text{Na}$.

Considering the limited substrate scope and non-negligible contribution from a non-catalyzed background radical trifluoromethylation of our protocol, our next target was to achieve a more selective and higher-yielding C–H bond trifluoromethylation of a wider range of substrates by utilizing the Umemoto reagent **A** as both a CF_3 source and oxidant. Although Umemoto reagents are relatively expensive, the ability to selectively trifluoromethylate C–H bonds using a simple and accessible Ni catalyst and a versatile reaction protocol (i.e., using either substrate or Umemoto reagent as a limiting reagent) may provide additional benefits when compared to existing trifluoromethylation methods where an excess of a substrate relative to the Umemoto reagent is always required. The resulting low conversion means that existing methods present a significant disadvantage for expensive substrates and natural products that may only be available only in small amounts.

After initial optimization (Table S4) using 3-methylindole as a model substrate, we found that trifluoromethylation catalyzed by 5 mol% of **3a** in the presence of 3 equiv of Umemoto reagent gives the product in 99% NMR and 92% isolated yields. Alternatively, the same quantitative 99% NMR yield is obtained when using the

Umemoto reagent as a limiting reagent with 3 equiv of 3-methylindole (Table S4, entry 10), similar to the protocol used by Sanford et al. for Ni-catalyzed trifluoromethylation with 2,8-difluoro-5-(trifluoromethyl)-5H-dibenzo[*b,d*]thiophen-5-ium trifluoromethanesulfonate.^[16a] We found that trifluoromethylation also occurs in MeOH, MeCN, and acetone, albeit in lower yields (56–72%) when compared to DMSO. The trifluoromethylation under nickel-free conditions, in the presence of 10 mol% of **L3**, showed no appreciable catalytic activity for the free ligand alone (Table S5 in the SI).

Finally, our optimized protocol was applied to a range of electron-rich arenes (**m–t**) and pharmaceutically active molecules (Scheme 5). For example, tadalafil underwent trifluoromethylation at the 7-position of the indole backbone to afford the same fluorinated analog **r** earlier reported by the Sanford group using 5 equiv of substrate relative to the Umemoto reagent, however using excess substrate was not required in our protocol leading to higher arene conversion. Melatonin, a well-studied natural hormone, reacted to afford a single trifluoromethylated product (**q**). A natural product amino acid, Cbz-L-tryptophan, was also well-tolerated (**p**), demonstrating our protocol's potential utility in the late-stage functionalization of pharmaceutically active molecules. For several substrates such as resorcinol and indole, a minor monotrifluoromethylation isomer was present (see **t** and **u** in Scheme 5 with arrows indicating alternative trifluoromethylation sites), while for other challenging substrates the amount of alternative product did not generally exceed 5%.



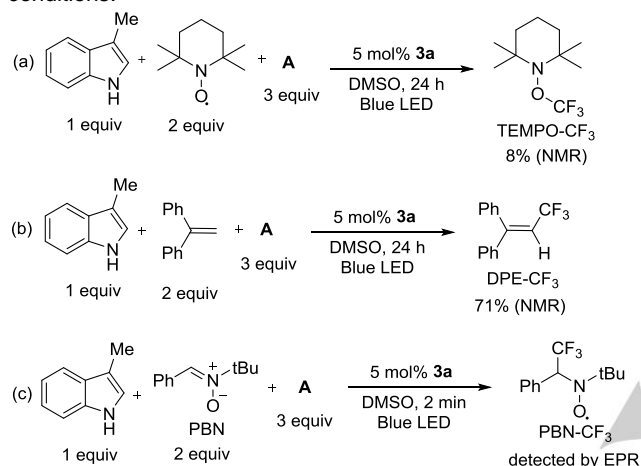
Scheme 5. Substrate scope of trifluoromethylation using Umemoto reagent.

Radical trap experiments. Although the Umemoto reagents are typically used as electrophilic trifluoromethylating reagents, examples of radical trifluoromethylation induced by single-electron transfer (SET) are also known. For example, Akita and co-workers described in detail a SET processes induced by light irradiation in the presence of common Ru or Ir photoredox catalysts, which led to one-electron reduction of the Umemoto

RESEARCH ARTICLE

reagent and generation of a CF_3 radical, which could further react with unsaturated substrates.^[35]

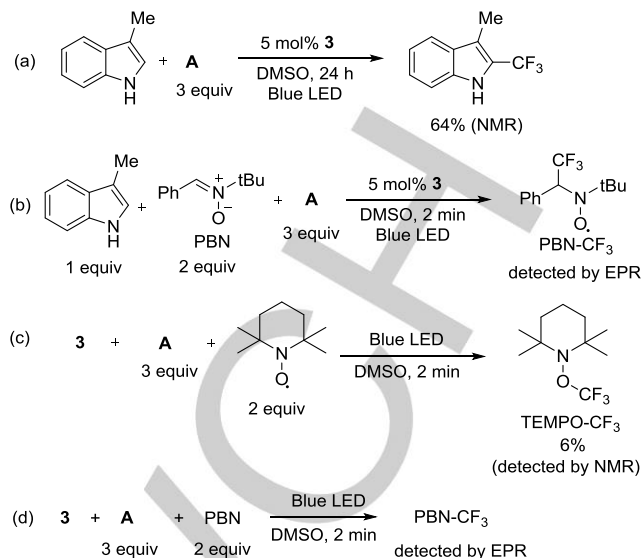
We thus set out to investigate whether CF_3 radical formation occurs under typical conditions for **3a**-catalyzed C–H trifluoromethylation in the presence of Umemoto reagent **A**, by using common radical traps (Scheme 6). The reaction between 3-methylindole and **A** catalyzed by **3a** under blue LED light was performed in the presence of TEMPO as the radical trap, and led to the formation of TEMPO-CF_3 , while product formation was inhibited. The formation of the trifluoromethyl radical was further confirmed via trapping it with 1,1-diphenylethylene (DPE) in 71% yield when analyzed by ^{19}F NMR spectroscopy and confirmed by HRMS analysis. Similarly, EPR spectroscopy was used to detect that PBN could be used to trap the CF_3 radical under catalytic conditions.



Scheme 6. Radical trap experiments under catalytic conditions. For experiments under light irradiation, 14 W blue LED lamp (465 nm) was used.

With the Umemoto protocol (where **A** can also act as an oxidant), we found that parent Ni^{II} complex **3** can also now act as a catalyst for the trifluoromethylation of 3-methylindole in the presence of 3 equiv of **A** under the standard conditions to give the trifluoromethylated product in 64% yield (Scheme 7, a).

Notably, this reactivity also involved CF_3 radical formation. The PBN-CF_3 adduct formed in the presence of PBN and substrate (Scheme 7, b). In the absence of substrate, we were also able to confirm the formation of CF_3 radical in the presence of **3**, 3 equiv of **A**, and TEMPO or PBN radical trap under blue LED irradiation, to give TEMPO-CF_3 or PBN-CF_3 adduct respectively (Scheme 7, c and d). This reactivity required light and no reaction was observed between **3** and **A** in the dark. The formation of **3a** by oxidation of **3** with **A** was also confirmed by the appearance of the characteristic purple color, and the resultant matching UV-vis absorption band, as well as ESI-HRMS, both in the absence and in the presence of 5 equiv of HBF_4 .

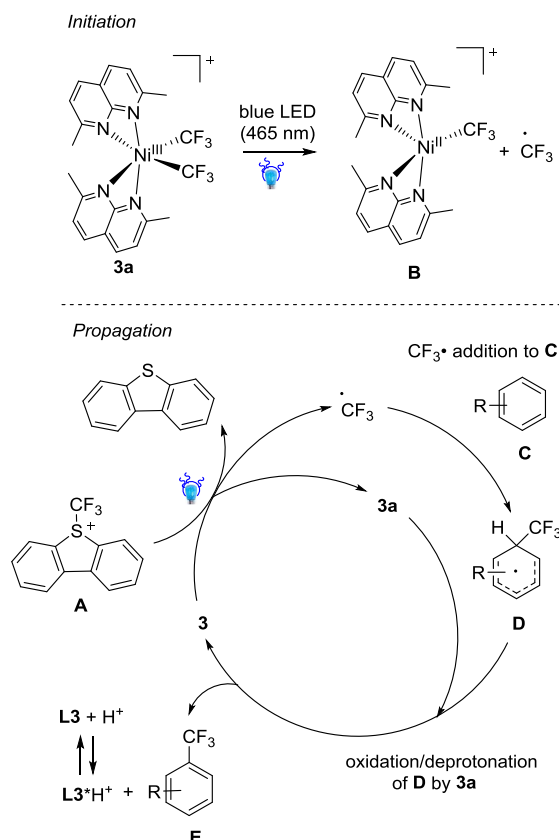


Scheme 7. Reactivity of **3** with the Umemoto reagent **A**. For experiments under light irradiation, 14 W blue LED lamp (465 nm) was used.

Based on these preliminary observations, we propose the following mechanism (Scheme 8). The initiation step involves $\text{Ni}^{\text{III}}\text{-CF}_3$ homolysis from catalyst **3a** to generate Ni^{II} complex **B** and a CF_3 radical; the latter then reacts with an aromatic substrate **C** to form intermediate **D**. Oxidation/deprotonation of **D** by another molecule of **3a** gives the trifluoromethylation product **E**; a free ligand equivalent released during reduction of **3a** to **3** may assist in deprotonation of **D**. One-electron reduction of **A** with **3** then generates a CF_3 radical which can further react directly with the aromatic substrate, or alternatively may react to regenerate **3a** from **B**. The protonated ligand is likely able to recombine with the complex during these $1e^-$ redox transformations since the solvent, DMSO, can assist with deprotonation.

Thus, we propose that **3a** acts as an initiator, which might lead to its partial decomposition, although further reactivity with Umemoto reagent might lead to some catalyst recovery. However, we have also shown that the catalytic cycle may be initiated directly by using **3** in catalytic amounts (Scheme 7, a) leading to a qualitatively similar result and confirming that the catalytic cycle could operate via $\text{Ni}^{\text{II}}/\text{Ni}^{\text{III}}$ redox transformations. Further studies are underway to clarify the role of the Ni complexes in different oxidation states in photocatalyzed trifluoromethylation.

RESEARCH ARTICLE



Scheme 8. Proposed radical pathway for trifluoromethylation using Umemoto reagent A.

The proposed mechanism in Scheme 8 implies that acidification of the reaction mixture should occur since no base was added. This was confirmed by pH measurements after the reaction, showing a weakly acidic media due to acid build-up. A similar effect could also be present in other reported examples of Ni-catalyzed trifluoromethylation using Umemoto-type reagents. Although this could eventually limit the overall TON, complex **3a** shows good stability even in the presence of a large excess of strong acid (up to 5200 equiv) under ambient conditions.

Overall, although the mechanism of trifluoromethylation catalyzed by **3a** will need to be further investigated in greater detail, these preliminary experiments show that the Umemoto reagent likely serves as the CF_3^\bullet radical source, rather than an electrophilic reagent, and light-induced one-electron redox transformations mediated by **L3**-supported Ni complexes are involved in the catalytic turnover.

Conclusion

In summary, we developed three bench-stable $\text{Ni}^{\text{III}}\text{-CF}_3$ complexes with a simple naphthyridine ligand using air as an oxidant. We showed that using blue light promotes catalytic C–H trifluoromethylation of heterocycles using either a radical or an electrophilic CF_3 source. This method is easy to set up, does not require a complicated or expensive protocol, and it is also efficient and can be performed under mild conditions. Preliminary mechanistic studies suggest that catalysis proceeds via a radical

mechanism and that a Ni^{IV} oxidation state may not be involved. Considering the increased interest in late-stage trifluoromethylation of natural products, future work will investigate the use of aliphatic substrates for trifluoromethylation involving $\text{Ni}^{\text{III}}\text{-CF}_3$ complexes.

Acknowledgements

R. R. F. performed crystal structure determination within the statements for Kazan Scientific Center of RAS. We thank Instrumental Analysis Section and Engineering Support Section for technical support and Scientific Computing and Data Analysis Section for access to HPC Cluster. The authors acknowledge the Okinawa Institute of Science and Technology Graduate University for funding.

Keywords: nickel • trifluoromethylation • C–H bond functionalization • radical formation • photoreactivity

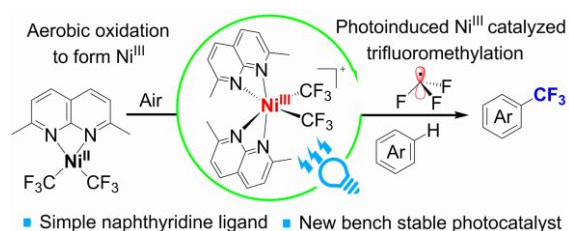
- [1] a) V. P. Ananikov, *ACS Catal.* **2015**, *5*, 1964–1971; b) S. Z. Tasker, E. A. Standley, T. F. Jamison, *Nature* **2014**, *509*, 299–309.
- [2] J. P. Stambuli, R. Kuwano, J. F. Hartwig, *Angew. Chem. Int. Ed.* **2002**, *41*, 4746–4748.
- [3] W. Guo, A. Cai, J. Xie, A. W. Kleij, *Angew. Chem. Int. Ed.* **2017**, *56*, 11797–11801.
- [4] a) E. J. Cho, T. D. Senecal, T. Kinzel, Y. Zhang, D. A. Watson, S. L. Buchwald, *Science* **2010**, *328*, 1679; b) A. R. Mazzotti, M. G. Campbell, P. Tang, J. M. Murphy, T. Ritter, *J. Am. Chem. Soc.* **2013**, *135*, 14012–14015; c) M. H. Katcher, A. Sha, A. G. Doyle, *J. Am. Chem. Soc.* **2011**, *133*, 15902–15905.
- [5] a) X. Hu, *Chem. Sci.* **2011**, *2*, 1867–1886; b) V. B. Phapale, D. J. Cárdenas, *Chem. Soc. Rev.* **2009**, *38*, 1598–1607; c) V. Snieckus, C. Allais, *Synfacts* **2017**, *13*, 0138–0138; d) X. Gao, Y. Geng, S. Han, A. Liang, J. Li, D. Zou, Y. Wu, Y. Wu, *Tetrahedron Lett.* **2018**, *59*, 1551–1554.
- [6] a) J. R. Bour, N. M. Camasso, M. S. Sanford, *J. Am. Chem. Soc.* **2015**, *137*, 8034–8037; b) N. M. Camasso, M. S. Sanford, *Science* **2015**, *347*, 1218; c) N. Nebra, *Molecules* **2020**, *25*.
- [7] F. Le Vaillant, E. J. Reijerse, M. Leutzsch, J. Cornella, *J. Am. Chem. Soc.* **2020**, *142*, 19540–19550.
- [8] B. Zheng, F. Tang, J. Luo, J. W. Schultz, N. P. Rath, L. M. Mirica, *J. Am. Chem. Soc.* **2014**, *136*, 6499–6504.
- [9] E. Chong, J. W. Kampf, A. Ariafard, A. J. Canty, M. S. Sanford, *J. Am. Chem. Soc.* **2017**, *139*, 6058–6061.
- [10] a) Y. Aihara, N. Chatani, *J. Am. Chem. Soc.* **2014**, *136*, 898–901; b) Z. Ruan, S. Lackner, L. Ackermann, *Angew. Chem. Int. Ed.* **2016**, *55*, 3153–3157; c) J. Xu, L. Qiao, J. Shen, K. Chai, C. Shen, P. Zhang, *Org. Lett.* **2017**, *19*, 5661–5664; d) S.-K. Zhang, R. C. Samanta, N. Sauermann, L. Ackermann, *Chem. Eur. J.* **2018**, *24*, 19166–19170; e) T. T. Tsou, J. K. Kochi, *J. Am. Chem. Soc.* **1978**, *100*, 1634–1635; f) M. Rovira, S. Roldán-Gómez, V. Martín-Diaconescu, C. J. Whiteoak, A. Company, J. M. Luis, X. Ribas, *Chem. Eur. J.* **2017**, *23*, 11662–11668.
- [11] C. Zhang, *Org. Biomol. Chem.* **2014**, *12*, 6580–6589.
- [12] L. Amini-Rentsch, E. Vanoli, S. Richard-Bildstein, R. Marti, G. Vilé, *Ind. Eng.* **2019**, *58*, 10164–10171.
- [13] S. Purser, P. R. Moore, S. Swallow, V. Gouverneur, *Chem. Soc. Rev.* **2008**, *37*, 320–330.
- [14] a) K. Müller, C. Faeh, F. Diederich, *Science* **2007**, *317*, 1881; b) W. K. Hagmann, *J. Med. Chem.* **2008**, *51*, 4359–4369.
- [15] D. A. Nagib, D. W. C. MacMillan, *Nature* **2011**, *480*, 224–228.

RESEARCH ARTICLE

- [16] a) E. A. Meucci, S. N. Nguyen, N. M. Camasso, E. Chong, A. Ariafard, A. J. Canty, M. S. Sanford, *J. Am. Chem. Soc.* **2019**, *141*, 12872-12879; b) X. Gao, Y. Geng, S. Han, A. Liang, J. Li, D. Zou, Y. Wu, Y. Wu, *Org. Lett.* **2018**, *20*, 3732-3735.
- [17] a) G. G. Dubinina, W. W. Brennessel, J. L. Miller, D. A. Vivic, *Organometallics* **2008**, *27*, 3933-3938; b) B. Vabre, P. Petiot, R. Declercq, D. Zargarian, *Organometallics* **2014**, *33*, 5173-5184; c) J. Hao, B. Vabre, D. Zargarian, *Organometallics* **2014**, *33*, 6568-6576.
- [18] F. D'Accrisio, P. Borja, N. Saffon-Merceron, M. Fustier-Boutignon, N. Mézailles, N. Nebra, *Angew. Chem. Int. Ed.* **2017**, *56*, 12898-12902.
- [19] S. T. Shreiber, D. A. Vivic, *Angew. Chem. Int. Ed.* **2021**, <https://doi.org/10.1002/anie.202104559>.
- [20] a) S. K. Kariofillis, A. G. Doyle, *Acc. Chem. Res.* **2021**, *54*, 988-1000; b) B. J. Shields, A. G. Doyle, *J. Am. Chem. Soc.* **2016**, *138*, 12719-12722; c) Z. Zuo, D. T. Ahneman, L. Chu, J. A. Terrett, A. G. Doyle, D. W. C. MacMillan, *Science* **2014**, *345*, 437; d) C. L. Joe, A. G. Doyle, *Angew. Chem. Int. Ed.* **2016**, *55*, 4040-4043; e) D. T. Ahneman, A. G. Doyle, *Chem. Sci.* **2016**, *7*, 7002-7006.
- [21] a) S. Deolka, O. Rivada-Wheelaghan, S. L. Aristizábal, R. R. Fayzullin, S. Pal, K. Nozaki, E. Khaskin, J. R. Khusnutdinova, *Chem. Sci.* **2020**, *11*, 5494-5502; b) O. Rivada-Wheelaghan, S. L. Aristizábal, J. López-Serrano, R. R. Fayzullin, J. R. Khusnutdinova, *Angew. Chem. Int. Ed.* **2017**, *56*, 16267-16271; c) O. Rivada-Wheelaghan, A. Comas-Vives, R. R. Fayzullin, A. Lledós, J. R. Khusnutdinova, *Chem. Eur. J.* **2020**, *26*, 12168-12179.
- [22] a) A. Okuniewski, D. Rosiak, J. Chojnacki, B. Becker, *Polyhedron* **2015**, *90*, 47-57; b) D. Rosiak, A. Okuniewski, J. Chojnacki, *Polyhedron* **2018**, *146*, 35-41.
- [23] Y. Yamaguchi, H. Ichioka, A. Klein, W. W. Brennessel, D. A. Vivic, *Organometallics* **2012**, *31*, 1477-1483.
- [24] Deposition Numbers 2092535-2092540 contain the supplementary crystallographic data for this paper. These data are provided free of charge by the joint Cambridge Crystallographic Data Centre and Fachinformationszentrum Karlsruhe Access Structures service www.ccdc.cam.ac.uk/structures.
- [25] C.-P. Zhang, H. Wang, A. Klein, C. Biewer, K. Stirnat, Y. Yamaguchi, L. Xu, V. Gomez-Benitez, D. A. Vivic, *J. Am. Chem. Soc.* **2013**, *135*, 8141-8144.
- [26] D. E. Hamilton, R. S. Drago, J. Telser, *J. Am. Chem. Soc.* **1984**, *106*, 5353-5355.
- [27] E. Lamour, S. Routier, J.-L. Bernier, J.-P. Catteau, C. Bailly, H. Vezin, *J. Am. Chem. Soc.* **1999**, *121*, 1862-1869.
- [28] S. Lapointe, E. Khaskin, R. R. Fayzullin, J. R. Khusnutdinova, *Organometallics* **2019**, *38*, 4433-4447.
- [29] J.-D. Chai, M. Head-Gordon, *PCCP* **2008**, *10*, 6615-6620.
- [30] F. Weigend, R. Ahlrichs, *PCCP* **2005**, *7*, 3297-3305.
- [31] C. F. Harris, C. S. Kuehner, J. Bacsa, J. D. Soper, *Angew. Chem. Int. Ed.* **2018**, *57*, 1311-1315.
- [32] J. R. Khusnutdinova, N. P. Rath, L. M. Mirica, *J. Am. Chem. Soc.* **2010**, *132*, 7303-7305.
- [33] a) B. R. Langlois, E. Laurent, N. Roidot, *Tetrahedron Lett.* **1991**, *32*, 7525-7528; b) Y. Ji, T. Brueckl, R. D. Baxter, Y. Fujiwara, I. B. Seiple, S. Su, D. G. Blackmond, P. S. Baran, *PNAS* **2011**, *108*, 14411; c) Y. Fujiwara, J. A. Dixon, F. O'Hara, E. D. Funder, D. D. Dixon, R. A. Rodriguez, R. D. Baxter, B. Herlé, N. Sach, M. R. Collins, Y. Ishihara, P. S. Baran, *Nature* **2012**, *492*, 95-99.
- [34] a) L. D. Haire, P. H. Krygsman, E. G. Janzen, U. M. Oehler, *J. Org. Chem.* **1988**, *53*, 4535-4542; b) E. G. Janzen, B. J. Blackburn, *J. Amer. Chem. Soc.* **1968**, *90*, 5909-5910; c) M. Danilczuk, F. D. Coms, S. Schlick, *Fuel Cells* **2008**, *8*, 436-452.
- [35] T. Koike, M. Akita, *Acc. Chem. Res.* **2016**, *49*, 1937-1945.

RESEARCH ARTICLE

Entry for the Table of Contents



Nickel complexes with simple naphthyridine ligands undergo facile aerobic oxidation to stable, isolated Ni^{III} organometallic complexes, in which $\text{Ni}-\text{CF}_3$ bond homolysis is observed upon blue LED light irradiation. These complexes catalyze photoinduced C-H bond trifluoromethylation in arenes and heteroarenes.

Institute and/or researcher Twitter usernames: [@KhusnutdinovaU](#)